Australian Journal of Earth Sciences (2006) **53**, (595–604)

Insights into the structure of the upper mantle beneath the Murray Basin from 3D teleseismic tomography

N. RAWLINSON*, B. L. N. KENNETT AND M. HEINTZ

Research School of Earth Sciences, Australian National University, ACT 0200, Australia.

Distant earthquake records from a passive array of 20 short-period seismometers are used to image the 3D P-wave velocity structure of the upper mantle beneath the Murray Basin in southern New South Wales and northern Victoria. During the five-month deployment period of the array, 158 teleseisms with good signal-to-noise ratios were recorded, allowing 3085 relative arrival time residuals to be picked with high accuracy. These arrival time residuals are mapped as 3D perturbations in P-wave velocity with respect to the *ak*135 global reference model using teleseismic tomography. The resulting images exhibit lateral variations in wave speed in the upper mantle to depths of nearly 300 km, and help to reveal the deep structure beneath a region almost devoid of Palaeozoic outcrop. Of particular significance is an east–west high–low–high relative wave speed variation that is present throughout the upper mantle between 70 and 250 km depth. The transition from faster to slower wave speeds in the west is indicative of a change from Proterozoic to Phanerozoic lithosphere that has also been observed further south in a previous teleseismic study. The transition from slower to faster wave speeds in the east has a less obvious association, but may well signal an underlying change in lithospheric structure related to the convergence of the western and central Lachlan subprovinces. At shallower depths (<70 km), the structural pattern is dominated by a fast perturbation (>3.5%) which overlies the slower region across the northern margin of the Bendigo Zone, and may be a consequence of localised thrusting and emplacement of denser lithosphere during the Early–Middle Devonian Tabberabberan Orogeny.

KEY WORDS: Delamerian Orogen, Lachlan Orogen, Murray Basin, teleseismic tomography, upper mantle.

INTRODUCTION

The Murray Basin in southeast Australia began to form in the Early Tertiary (Lawrence & Abele 1988), with subsequent sedimentary deposition obscuring large regions of the underlying Palaeozoic terrane, which is of key importance in unravelling the tectonic assemblage of eastern Australia. In particular, the presence of young cover sequences has inhibited a more complete understanding of the evolution of the Lachlan Orogen, which represents much of the southern Tasmanides. To date, a wide variety of models have been developed to explain the tectonic setting of the Lachlan Orogen, ranging from a predominantly accretionary oceanic system (Foster & Gray 2000; Fergusson 2003; Spaggiari *et al.* 2003, 2004) to a largely intracratonic model (VandenBerg 1999; Taylor & Cayley 2000; Willman *et al.* 2002).

In this paper, teleseismic tomography is used to image the upper mantle P-wave velocity structure beneath the Murray Basin in northern Victoria and southern New South Wales, which incorporates much of the western subprovince of the Lachlan Orogen. Teleseismic tomography uses relative arrival times from distant earthquake sources, recorded across an array of seismic stations, to image the seismic structure of the upper mantle. It has been frequently used in various parts of the world (Aki *et al.* 1977; Oncescu *et al.* 1984; Humphreys & Clayton 1990; Achauer 1994; Steck *et al.* 1998; Lippitsch *et al.* 2003) but has seen little application in Australia. High seismicity along the margins of the Australian Plate, particularly in the north and east, makes the southeast region of Australia an ideal natural laboratory for passive array experiments using distant earthquake sources. Recently, teleseismic tomography studies have been carried out in western Victoria (Graeber *et al.* 2002) and northern Tasmania (Rawlinson *et al.* 2006); in the former case, the array is adjacent to the one in this study, which allows a comparison of results.

The use of distant earthquake sources combined with the geometry of our seismic array permits large-scale upper mantle features (upwards of 50 km across) to be imaged, but not short-wavelength crustal anomalies. While this limits the ability of our results to directly address some of the controversies regarding the tectonic evolution of the Lachlan Orogen, valuable insights can nonetheless be gained from the illumination of deeper mantle features. These could include, for example, boundaries between compositionally distinct lithosphere

*Corresponding author: nick@rses.anu.edu.au

ISSN 0812-0099 print/ISSN 1440-0952 online © Geological Society of Australia
DOI: 10.1080/08120090600686751

(Graeber *et al.* 2002) or remnants of subducted material preserved in the lithosphere from past orogens (Calvert *et al.* 1995).

Another factor that needs to be considered when interpreting our seismic imaging results is the relationship between seismic-wave speed and the chemical and physical properties of the medium through which the waves propagate. Seismic P-wave perturbations (i.e. departures from a spherically symmetric earth model) in the upper mantle are largely a function of variations in temperature, composition, the presence of melt, solid phase transformations and anisotropy, although it is generally thought that in most cases temperature and composition are the two principal factors (Sobolev *et al.* 1996). According to Cammarano *et al.* (2003), a 100°C increase in temperature at 200 km depth can produce a negative P-wave velocity anomaly of up to nearly 1%. The effects of composition are more contentious, with maximum estimates for wave-speed perturbations as a result of realistic variations in mantle composition ranging between 1 and 5% (Sobolev *et al.* 1996; Griffin *et al.* 1998; Cammarano *et al.* 2003). A P-wave velocity model alone does not contain sufficient information to discriminate between contributions from temperature and composition, which means that caution is required when attempting to identify the underlying cause for the presence of a velocity anomaly.

SEAL EXPERIMENT AND DATA

The South East Australia Linkage (SEAL) experiment is a passive seismic array study of southern New South Wales and northern Victoria undertaken by the Research School of Earth Sciences at the Australian National University. SEAL commenced with the deployment of 20 vertical-component short-period seismometers in early November 2004 using a station spacing of 50–80 km (Figure 1a). All instruments were retrieved in early April 2005, resulting in a five-month deployment period during which numerous teleseisms were recorded. In addition to allowing a significant portion of the Lachlan Orogen beneath the Murray Basin to be imaged using teleseismic tomography, SEAL also forms a geographic link between several past and future high-density array studies in the region [including LF98 (1998), MB99 (1999), QUOLL (1999), AF00 (2000), EVA (2005–2006): Figure 2].

Of the numerous events recorded by SEAL, a subset of 158 teleseisms with good signal-to-noise ratios was selected for picking. Figure 1b shows the distribution of these events on an equidistant projection centred on the array. The azimuthal coverage is good from the northwest to the east of the array, with many events occurring in the Andaman Islands, northern Sumatera, Mindanao, Japan, the Solomon Islands, Fiji and Tonga. However, far fewer events were detected from the south and west, which means that ray-path coverage beneath the SEAL array will be dominated by events from the north and east. While this will affect the recovery of structure, further investigation into the potential resolving power of the dataset will be postponed to the results section (below) where a checkerboard resolution test is carried out.

Most of the phases picked from the 158 teleseisms are direct P phases, which turn back to the surface from within the mantle and represent the first arriving phase of the teleseismic wave-train. However, we have been able to pick a relatively small number of other phases, including PP (reflection from the free surface), PcP (reflection from the outer core), ScP (converted reflection from the outer core), and PKiKP (reflection from

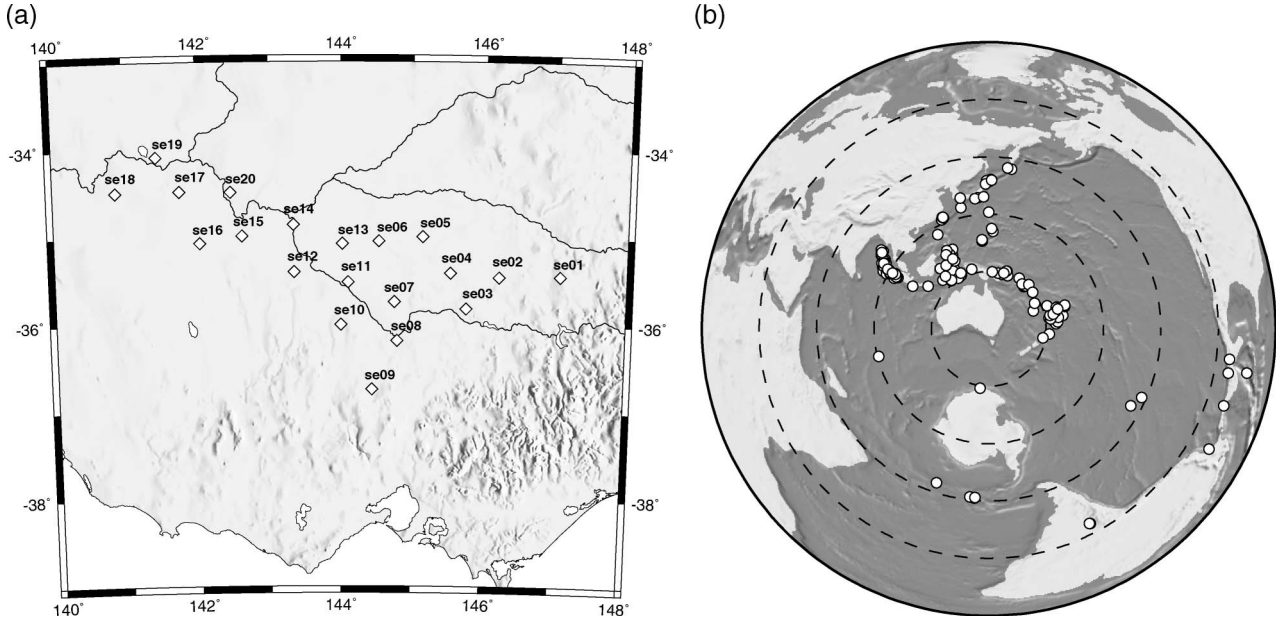

Figure 1 (a) Locations of the 20 short-period stations that comprise the SEAL seismic array in southern New South Wales and northern Victoria. (b) Distribution of 158 teleseismic events used in the tomographic inversion for the 3D seismic structure beneath the Murray Basin. Dashed circles represent equidistant curves from the centre of the SEAL array at 30° increments.

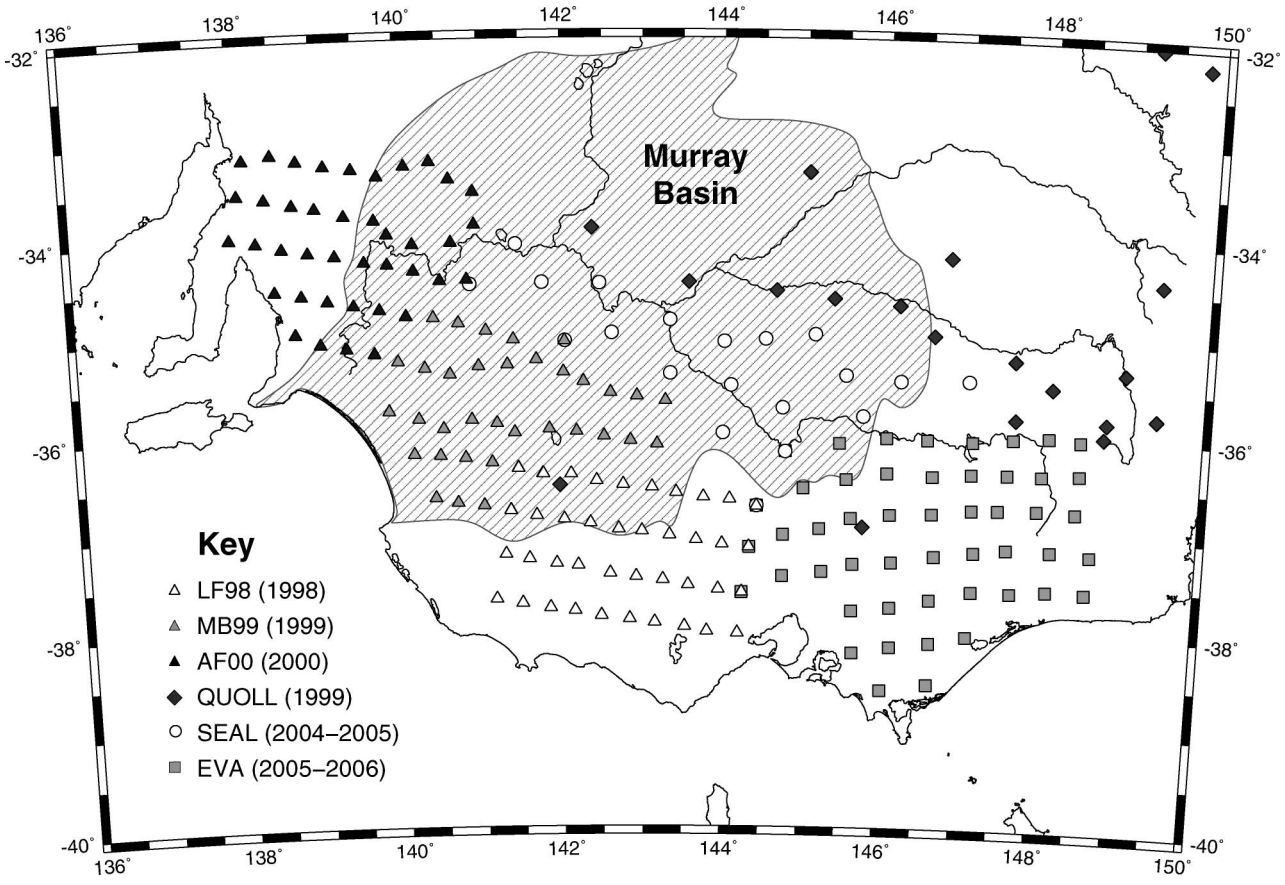

Figure 2 Location of recent and current passive seismic arrays deployed in southeast Australia. The approximate coverage of the Murray Basin is also shown.

the inner core). A number of events from central America (Figure 1b) produced particularly clear PKiKP arrivals.

Once a phase is identified in the data, all traces are approximately aligned using moveout corrections from the *ak*135 global reference model (Kennett *et al.* 1995). Figure 3 shows phases from two different events that have been aligned using this procedure. Any remaining misalignment between traces can be attributed largely to lateral variations in wave speed in the upper mantle beneath the array. In order to extract these so-called arrival-time residuals, the semi-automated adaptive stacking technique of Rawlinson and Kennett (2004) is used. This scheme is able to produce robust and accurate estimates of arrival-time residuals by exploiting the relative invariance in shape (or coherence) of teleseismic waveforms recorded at nearby stations. Error estimates for the picking are also produced, which are used to weight the relative importance of each residual in the subsequent tomographic inversion. A total of 3085 arrival-time residuals are picked from the 158 events. In order to account for errors in source-origin time and large-scale variations in mantle structure outside the modelled region, the mean is removed from each residual set to produce relative arrival-time residuals. As a consequence, perturbations in wave speed recovered by the tomography should be viewed as relative rather than absolute.

Figure 4 shows the relative arrival-time residual patterns for each of the events shown in Figure 3 obtained using the adaptive stacking procedure. Note the coherent pattern of residuals in each case, which is suggestive of significant lateral variations in mantle structure beneath the array. Regions in which arrival-time residuals are negative suggest the presence of relatively fast lithosphere, and regions in which arrival-time residuals are positive suggest the presence of a relatively slow lithosphere. However, the path-integral nature of the residuals means that the pattern will change according to source location (cf. Figure 4a and b), so the only sensible way of interpreting these data is to map them as 3D variations in wave speed using teleseismic tomography.

TOMOGRAPHIC INVERSION SCHEME AND RESOLUTION TESTS

The standard approach to teleseismic tomography is to embed a local 3D model volume that lies beneath the receiver array within a global spherically symmetric reference model (Benz *et al.* 1992; Saltzer & Humphreys 1997; Frederiksen *et al.* 1998). This allows rapid travel-time predictions to be made from the source to the boundary of the local model before applying more sophisticated ray-tracing techniques for laterally

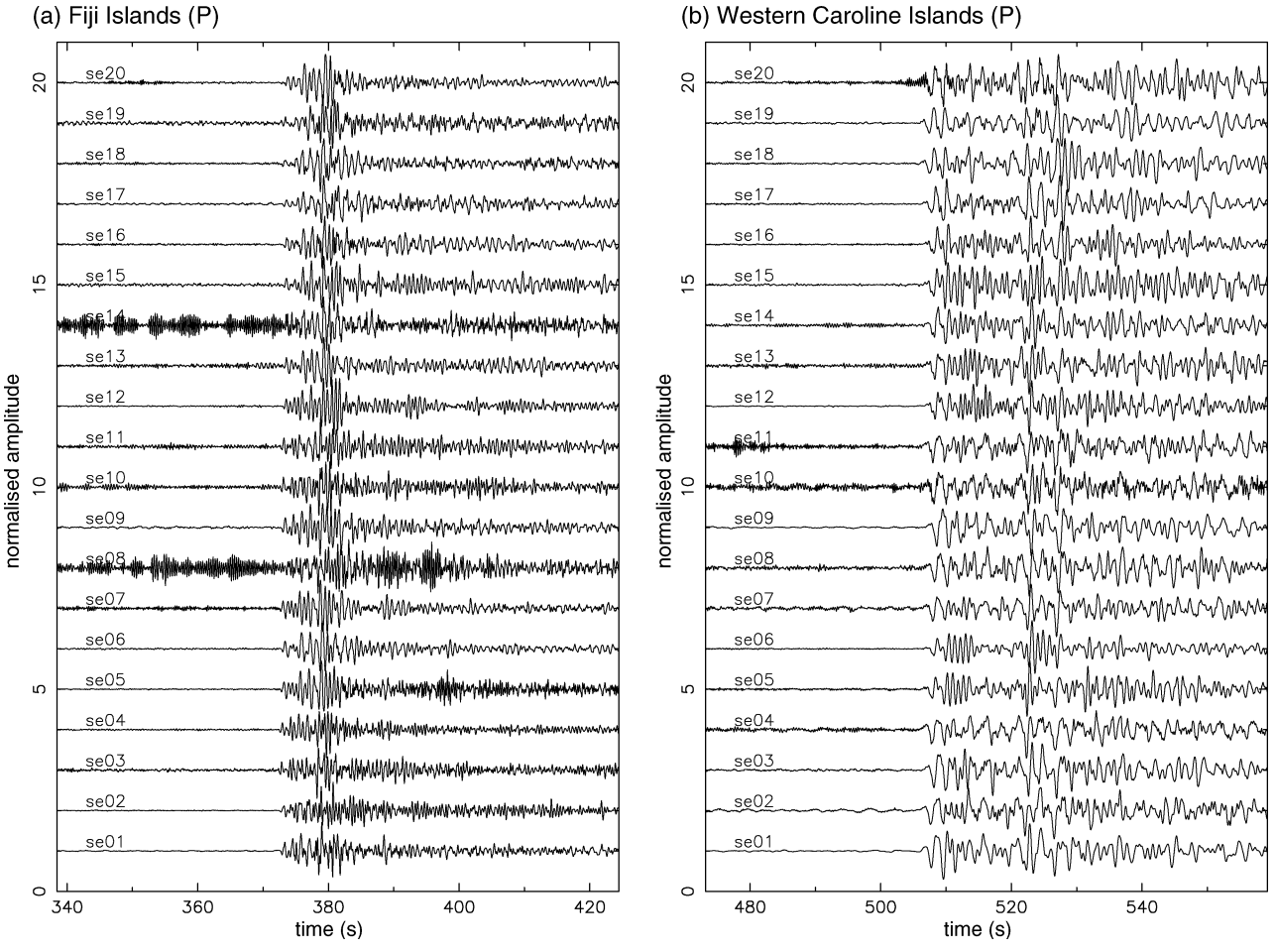

Figure 3 Records from the 20 SEAL stations for two different teleseismic events. Trace moveout has been corrected for using the *ak*135 global reference model. (a) m_b 6.6 event from the Fiji Islands which occurred on 17 November 2004. (b) m_b 6.6 event from the western Caroline Islands which occurred on 16 January 2005.

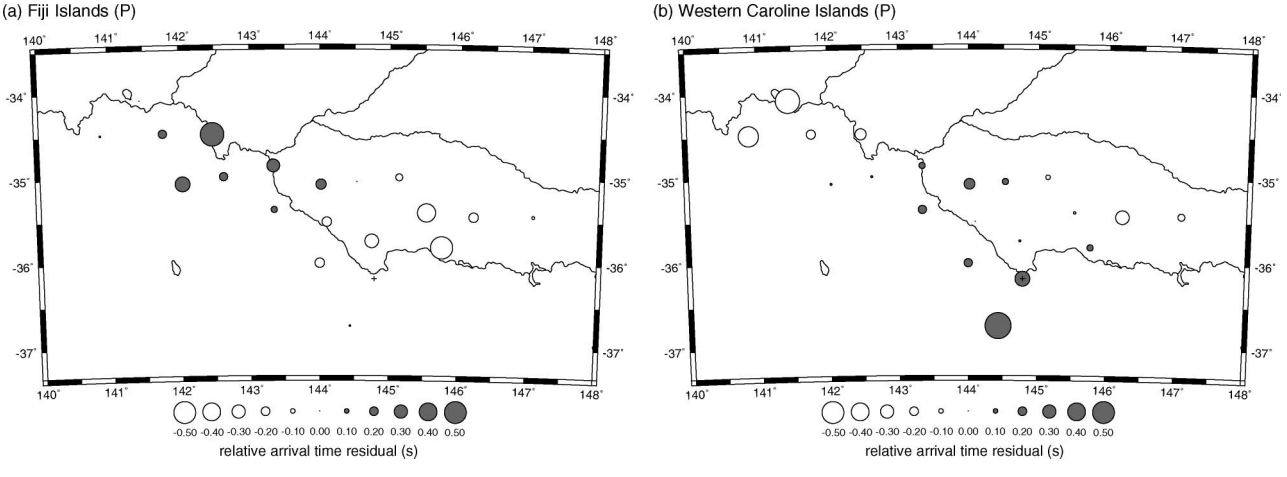

Figure 4 Relative arrival-time residual patterns for two different events obtained by aligning each set of traces shown in Figure 3 using the adaptive stacking technique of Rawlinson and Kennett (2004).

heterogeneous media. The key assumption of this approach is that lateral variations in structure outside the local model volume do not significantly affect relative arrival-time residual patterns.

A novel iterative non-linear tomographic procedure that combines both computational speed and robustness is used to map the relative arrival-time residual patterns as P-wave velocity anomalies. Structure within the local 3D model volume beneath the seismic array is represented using smoothly varying cubic B-spline volume elements, the values of which are controlled by a mesh of velocity nodes in spherical coordinates.

Travel times to the base of the local model from each source are computed through the *ak*135 global reference model using an efficient $\tau - p$ approach (Kennett & Engdahl 1991). A grid-based eikonal solver, known as the fast marching method (FMM), is used to compute travel times from the base of the model to the receiver array on the surface. The inverse problem requires adjustment of the velocity node values in order to match the predicted arrival-time residual patterns with the observed patterns, subject to regularisation constraints. This is solved using the subspace inversion method (Kennett *et al.* 1988), and we include both damping and smoothing regularisation to address the problem of solution non-uniqueness. The forward travel-time prediction and inversion steps are applied iteratively to account for the non-linearity of the tomographic inverse problem. Further details on the new scheme can be found in Rawlinson and Sambridge (2005) and Rawlinson *et al.* (2006).

In order to apply the tomographic inversion scheme to the SEAL dataset, the seismic structure beneath the 20 station array is represented using a local model volume comprising 21 645 velocity nodes at $\sim$25 km spacing in all three dimensions (latitude, longitude and depth). The model spans 300 km in depth, 8.13° in latitude and 12.78° in longitude. The 1D reference or starting model is given by *ak*135. Six iterations of the tomographic inversion scheme are applied to the 3085 relative arrival-time residuals to produce a solution model which satisfies the data to an acceptable level. The solution model reduces the data variance by 78% from 0.0397 s^2 to 0.0087 s^2, which corresponds to an RMS reduction from 199.3 ms to 93.3 ms. Figure 5a and b show histograms of the distribution of relative arrival time residuals for the initial and final model, respectively.

Before presenting the tomographic results, the robustness of the solution model is first investigated using synthetic checkerboard tests (Rawlinson & Sambridge 2003). These tests involve using the identical sources, receivers and phase types from the observational dataset to predict the arrival-time residuals for a synthetic structure comprising an alternating 3D pattern of fast and slow velocities. The predicted data are then inverted using the tomographic procedure outlined above, and the resulting differences between the synthetic and recovered structures give an indication of the resolution that can be achieved in each region of the model. Figure 6 shows a series of cross-sections through a synthetic checkerboard and the corresponding recovered model obtained using this procedure with the SEAL source and receiver geometry. Overall, the recovery of the pattern is good in regions of the model

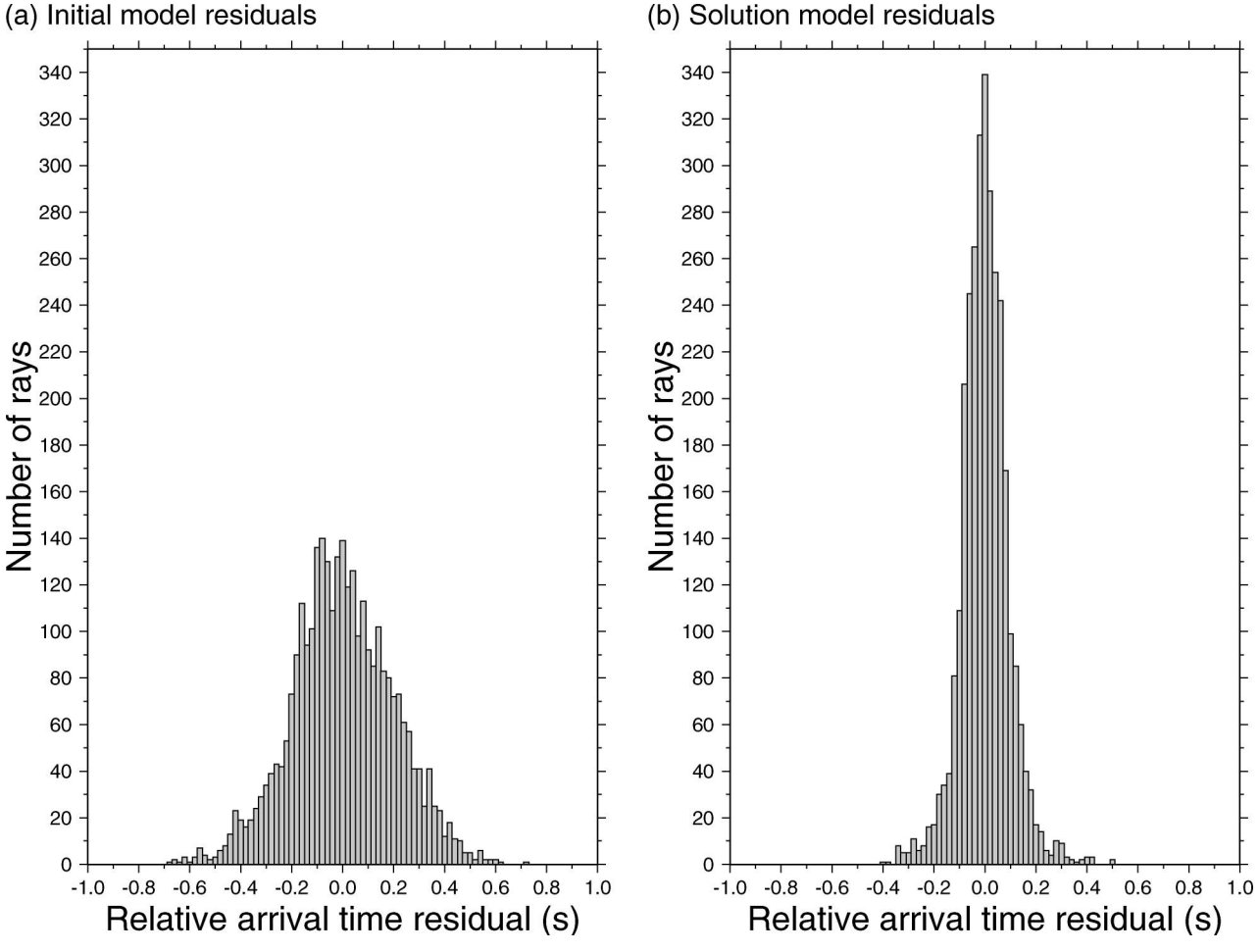

Figure 5 Magnitude and distribution of relative-arrival time residuals for (a) initial model and (b) solution model.

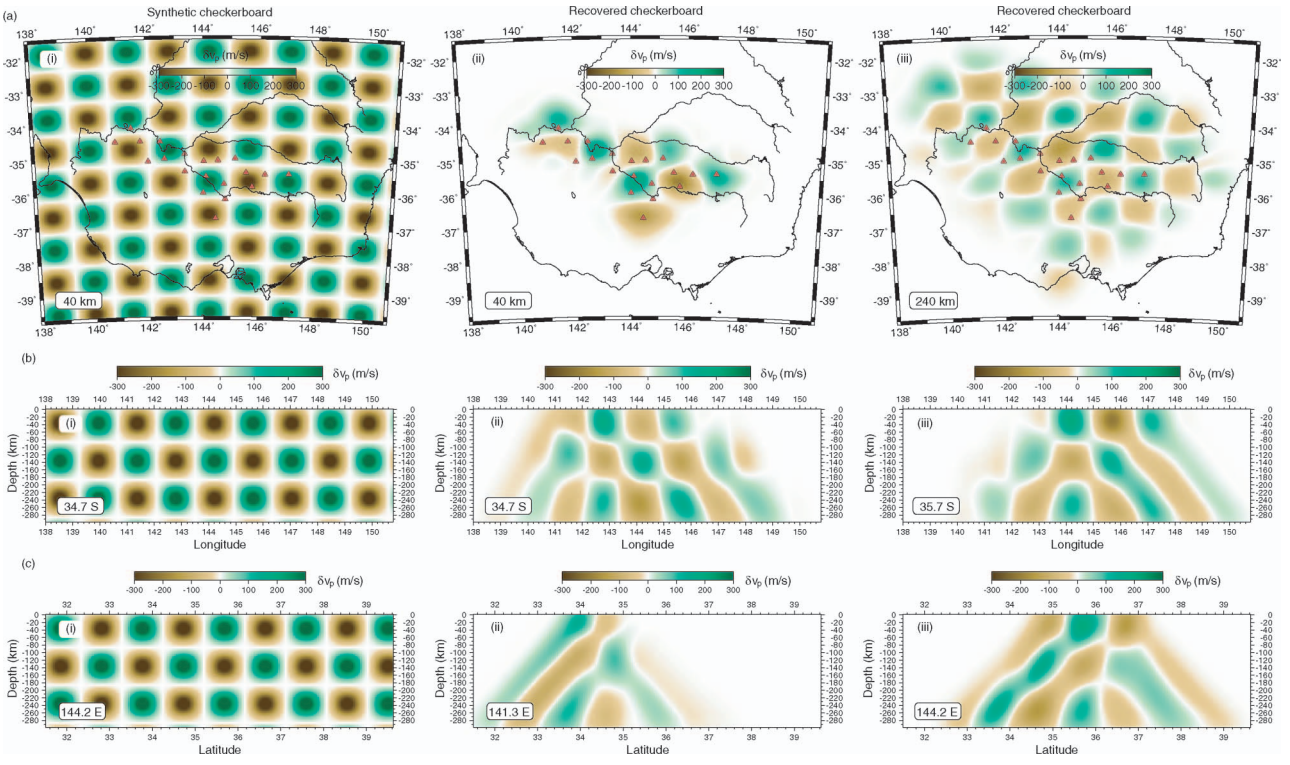

Figure 6 Input and recovered checkerboard models for synthetic resolution tests. (a) Depth slices. (b) East–west slices. (c) North–south slices. In each case, (left) input checkerboard; (centre and right) recovered checkerboards. Note that the checkerboard varies in all three dimensions, so slices with the same orientation taken at different places may have opposite polarities.

where ray-path coverage is dense. Due to the use of distant earthquake sources, ray paths converge beneath the receiver array from deep in the mantle, which means that a greater portion of the checkerboard pattern is recovered with increasing depth [cf. Figure 6a (ii) and (iii)].

The east–west cross-sections through the checkerboard inversion model (Figure 6b) generally exhibit good recovery, although there is some smearing of structure towards the edge of the array caused by a predominance of paths with similar orientations. The north–south cross-sections (Figure 6c) also recover some of the checkerboard pattern, although smearing is clearly evident beyond the horizontal bounds of the array. The minimum scale length of structure that can be recovered by the tomography is around 40–50 km, similar to the station spacing. This means that the large-amplitude short-wavelength velocity anomalies that are often encountered in the crust are unlikely to be imaged. In summary, the upper mantle structure appears to be well constrained by the path coverage, although resolution tends to decrease beyond the horizontal bounds of the seismic array.

TOMOGRAPHIC MODEL

Horizontal and vertical cross-sections through the SEAL tomographic model are shown in Figure 7 and exhibit a number of distinctive features. The major first-order structure appears to be an east–west fast–slow–fast relative variation in wave speed in the upper mantle below about 70 km depth. This variation can be seen in horizontal sections in Figure 7a (ii) and (iii), which show a zone of reduced velocity between about 143 and 146°E, bounded to both the west and east by regions of elevated velocity. The vertical east–west slice in Figure 7b (ii) clearly shows this region of lower velocity extending into the mantle to a depth of about 280 km. The checkerboard resolution tests [Figure 6b (ii)] indicate that this part of the model is well constrained by the data. The slices at 34.0°S and 35.7°S in Figure 7b also exhibit some evidence of the fast–slow–fast velocity feature, although there is a lack of resolution to the east of 144°E in Figure 7b (i) and to the west of 142°E in Figure 7b (iii), which makes it appear more nebulous. The three north–south slices in Figure 7c clearly highlight the presence of the east–west-trending fast–slow–fast pattern of velocity variation. The slice at 141.3°E is almost entirely fast; the slice at 144.0°E is predominantly slow (except for a distinct shallow fast anomaly); and the slice at 147.0°E is virtually all fast. However, it should be noted that the northern and southern extents of the faster zone in the east may be exaggerated somewhat by smearing effects caused by insufficient ray-path coverage beyond the horizontal bounds of the array.

Another prominent feature of the tomographic model is a fast shallow anomaly located above the slow anomaly beneath the centre of the array. It spans a region of about 143.5–145.5°E in longitude, 35–36°S in latitude and 0–70 km in depth [see Figure 7a (i), 7b (iii), 7c (ii)], and has a maximum perturbation in excess

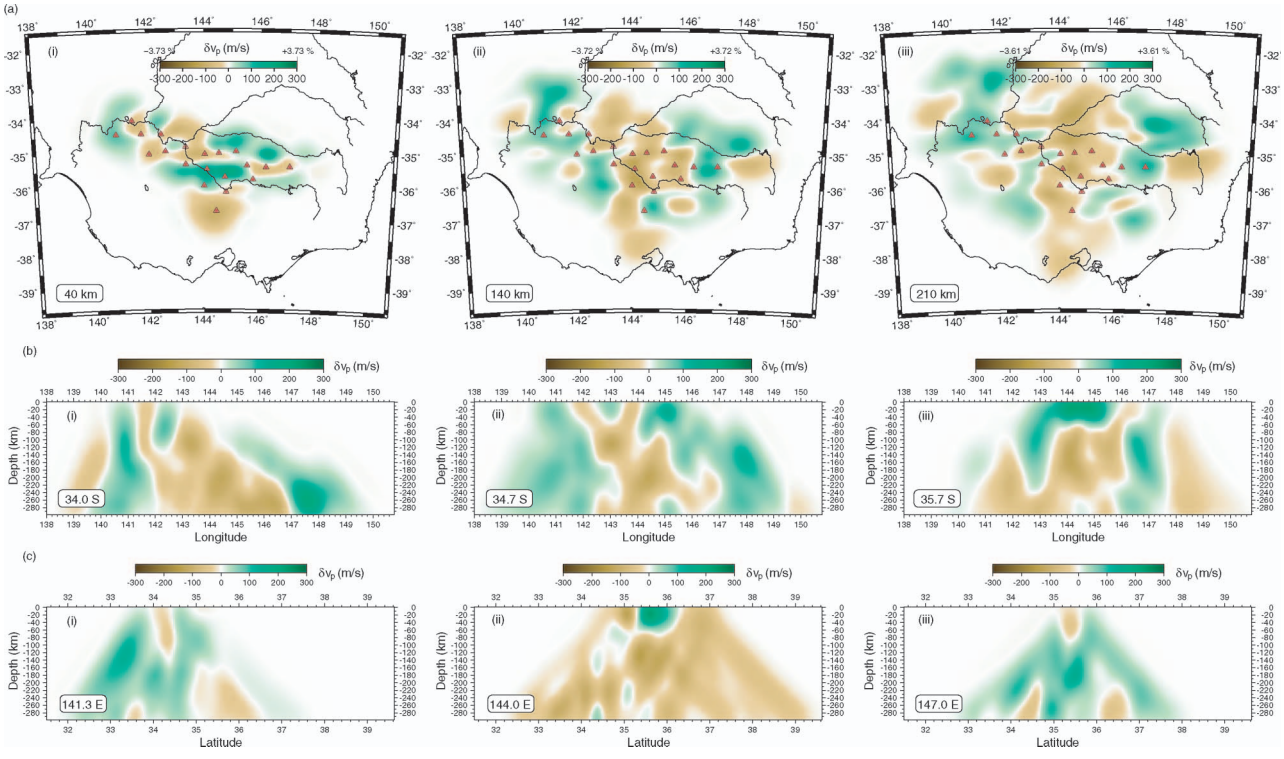

Figure 7 Horizontal and vertical slices through the 3D solution model obtained by inversion of SEAL dataset. (a) Depth slices. (b) East – west slices. (c) North – south slices.

of +3.5%, greater than any other feature recovered by the tomography. In considering the geological implications of this anomaly, it is worth remembering that crustal structure is generally not well resolved. Thus, contributions to relative arrival-time residuals made by lateral heterogeneity in the crust are likely to map as structure in the shallow mantle. It is therefore possible that a region of thinner crust or a shallow body of fast material within the crust has manifested as a prominent fast region of substantial thickness. However, there is little evidence from existing magnetic, gravity (VandenBerg *et al.* 2000) or receiver function derived crustal thickness data (Clitheroe *et al.* 2000) that supports the presence of a significant broad-scale anomaly in this region that is confined only to the crust.

The main features of the tomographic model described above constitute robust first-order structures that are well constrained by the teleseismic dataset. While other anomalies are also present in the model, they generally have a much smaller spatial extent, and we would caution the reader against excessive interpretation of such features in the absence of more extensive resolution tests. It is interesting to note that the magnitude and style of the major anomalies seen in our results are not unlike those inferred from teleseismic delay times further north in eastern Queensland (Hearn & Webb 1984).

DISCUSSION

The SEAL experiment has allowed the upper mantle beneath the Murray Basin in southeast Australia to be imaged in much greater detail than previous seismic studies. For example, the continent-wide deployment of portable broadband seismometers that includes SKIPPY and several subsequent experiments has allowed the upper mantle beneath all of Australia to be imaged using surface-wave tomography (Zielhuis & van der Hilst 1996; Debayle & Kennett 2000; Fishwick *et al.* 2005). However, the maximum horizontal resolution permitted by surface-wave tomography is around 200 km, which is much lower than for our targeted study. Consequently, several features observed in our models are not present in the surface-wave tomography results.

In 1998, Monash University and the University of Adelaide jointly deployed 40 short-period seismometers (the LF98 array) in western Victoria (Figure 2) to record distant earthquakes for subsequent interpretation by teleseismic tomography (Graeber *et al.* 2002). LF98 spanned the western end of the Lachlan Orogen and the Newer Volcanic Province, and lies to the south of the western half of the SEAL array; in fact, the southernmost SEAL station (se09) is co-located with the station lying at the northeastern corner of LF98 (Figure 2). The tomographic results from LF98 can therefore be meaningfully compared with the results in this paper, although it should be pointed out that there is a sizeable gap between the two arrays that widens in the westward direction from the co-located stations. Subsequent to the LF98 array, two more 40 station short-period arrays (MB99 and AF00) were deployed to the northwest (Figure 2), and fill in the gap between SEAL and LF98. However, results from these experiments are yet to be published.

One of the major upper mantle features imaged by the LF98 experiment is a strong velocity contrast, with

average velocities about 2% greater in the west, beneath the Moyston Fault Zone (Graeber *et al.* 2002) at about 37°S, to a depth of about 100 km. This has been interpreted by Graeber *et al.* (2002) as representing a lithospheric boundary between the Delamerian Orogen and the Lachlan Orogen. At greater depths, positive wave-speed anomalies persist to the north and east of this feature. The most likely explanation for the observed contrast in wave speed is in the compositional differences between the Proterozoic lithosphere that underpins the Delamerian Orogen and the younger Phanerozoic lithosphere that comprises the Lachlan Orogen, although some thermal contribution is also possible. According to Griffin *et al.* (1998), typical Archaean mantle lherzolites can have seismic P-wave speeds up to 5% greater than Phanerozoic mantle lherzolites, which tend to be far richer in clinopyroxene and CaO but relatively depleted in orthopyroxene. Although no estimate of P-wave speed is provided for Proterozoic mantle lherzolites, they are compositionally much more like the Archaean lherzolites than Phanerozoic lherzolites (Griffin *et al.* 1998), so presumably they share similar wave-speed characteristics.

A lack of resolution above 100 km depth at 37°S prevents the strong velocity contrast beneath the Moyston Fault Zone from being observed in the SEAL tomographic model, although there are clearly elevated wave speeds beneath the western end of the array contrasting with lower wave speeds beneath the centre of the array. Figure 8 shows a horizontal section through the solution model at 140 km depth with major structural boundaries derived from surface mapping and potential-field data (Foster & Gray 2000; Cayley *et al.* 2002; Willman *et al.* 2002) superimposed. The elevated velocities beneath the Stawell Zone correlate well with the location of the elevated velocities seen at this depth in the LF98 model and may well be caused by the presence of Precambrian basement extending beneath the western part of the Lachlan Orogen in the vicinity of the Murray Basin, as has previously been suggested by Zielhuis and van der Hilst (1996) and Simons *et al.* (1999) based on surface-wave tomography. The upper mantle beneath the Delamerian Orogen in Figure 8 is almost uniformly fast and contrasts with the slower velocities beneath most of the western Lachlan Orogen.

The relatively fast velocities observed beneath the Wagga – Omeo Complex (Figure 8) suggest that the upper mantle which underlies the central subprovince of the Lachlan Orogen is seismically distinct from the upper mantle beneath the western subprovince. It is interesting to note that surface-wave tomography does not detect elevated shear velocities in this region (Debayle & Kennett 2000; Fishwick *et al.* 2005), which means that the P-wave anomaly is quite localised (i.e. has a scale-length below the resolving power of surface-wave tomography) or is a zone of elevated V_p/V_s ratio. From the surface geology, the central subprovince represents the main concentration of Palaeozoic intermediate- to high-grade, low-pressure metamorphism in the Lachlan Orogen (Foster & Gray 2000). One possible model for the tectonic evolution of this region involves eastward subduction of oceanic lithosphere beneath an island-arc complex to form a high-temperature metamorphic/plutonic zone in the Late Ordovician, followed by juxtaposition of the Tabberabbera and Melbourne Zones as a consequence of double-divergent subduction (Foster & Gray 2000; Spaggiari *et al.* 2003). The elevated wave speeds observed in the upper mantle beneath the central subprovince (Figure 8) may therefore be a signature of remnant underplated oceanic lithosphere. However, if this was the case, the positive velocity anomaly would more likely be a consequence of decreased temperature rather than a change in composition (Cammarano *et al.* 2003). Note that there have been a number of previous seismic studies which have established that remnants of subducting slabs dating back from as far as the Archaean

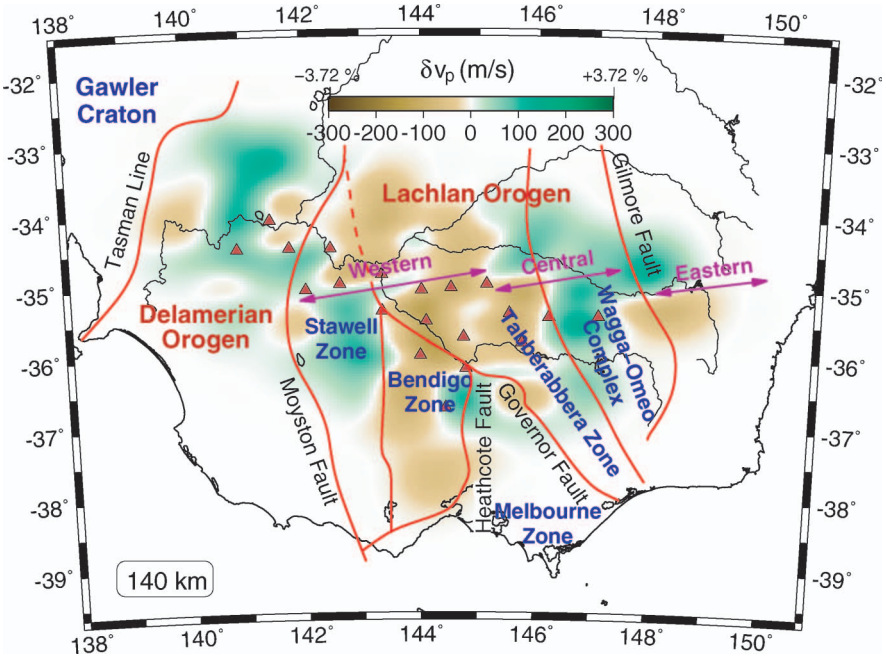

Figure 8 Slice through solution model at 140 km depth with a schematic map of major regions and boundaries of the southern Tasmanides superimposed.

can be preserved relatively intact within the lithospheric mantle (Calvert *et al.* 1995; Cook *et al.* 1999; Balling 2000; Hansen & Balling 2004).

An alternative explanation for the formation of the central subprovince involves major strike-slip motion between the so-called Whitelaw and Benambra Terranes in the vicinity of the present-day Governor Fault (Willman *et al.* 2002). In this model, the Whitelaw Terrane represents the western subprovince, and the Benambra Terrane represents the central and eastern subprovinces. Prior to the Early Silurian, the western part of the Benambra Terrane adjoined the Whitelaw Terrane to the north and shared a similar tectonic evolution. However, subsequent orogeny translated the Benambra Terrane some 600 km to the southeast along the Baragwanath transform (an inferred major fault), resulting in the current east–west juxtaposition of the two terranes. If a substantial region of the western Benambra Terrane was underlain by Proterozoic basement similar to that beneath the Delamerian Orogen prior to movement along the Baragwanath transform, then this model would also be consistent with our results.

The third feature of the tomographic model that should be noted is the shallow zone of relatively fast wave speed which crosses the Governor Fault at the northern end of the Bendigo Zone [Figure 7a (i), 7b (iii), 7c (ii)]. As noted previously, the depth extent of this structure is not well constrained by the data, so it may not be as extensive as suggested by the images. One possible explanation for the anomaly involves the allochthonous emplacement of mafic and ultramafic rocks (formed as a consequence of easterly subduction beneath the central subprovince) during the collision of the Melbourne and Tabberabbera Zones in the Early–Middle Devonian. This explanation appeals to the double divergent subduction models of Foster and Gray (2000) and Spaggiari *et al.* (2003), but given the limited constraints on the anomaly available from the tomography, other equally valid hypotheses could be formulated. Finally, the proposed existence of the Selwyn Block as Proterozoic basement beneath the Melbourne Zone (Cayley *et al.* 2002) cannot be verified by our results as the resolution of our model beneath this region is poor.

CONCLUSIONS

In this paper, we have presented recent results from teleseismic tomography of the upper mantle beneath the Murray Basin in northern Victoria and southern New South Wales. The transition from the Precambrian regions of central and western Australia to the Phanerozoic zones in the east is clearly revealed in our results by a change from higher velocities in the upper mantle beneath the Delamerian Orogen to lower velocities beneath much of the western subprovince of the Lachlan Orogen. However, the region of faster velocity extends beneath the central part of the Stawell Zone, which suggests that Proterozoic basement may extend eastward beneath some of the Lachlan Orogen. Higher velocities in the upper mantle beneath the Wagga–Omeo Complex may be due to the presence of remnant underplated oceanic lithosphere, although a model involving the transport and emplacement of Proterozoic lithosphere from the northwest could also be valid. A shallow region (<70 km deep) of elevated velocities to the north of the Bendigo Zone may be related to the juxtaposition of the Melbourne and Tabberabbera Zones in the Early–Middle Devonian. The deployment of a new passive seismic array in eastern Victoria in late September 2005 promises greater resolution of the transition between the Melbourne Zone, Tabberabbera Zone and Wagga–Omeo Complex south of the SEAL array. Our long-term goal is to combine data from the new array and all previous teleseismic experiments in southeast Australia to construct a unified tomographic model of the entire region.

ACKNOWLEDGEMENTS

We would like to thank Tony Percival, Armando Arcidiaco and Erdinc Saygin for assistance with the deployment of short-period seismometers in the field. We also thank the many private landowners for their generous permission in allowing us to install instruments on their property. The use of short-period seismic equipment from the ANSIR Major National Research Facility is gratefully acknowledged. D. Gray and S. Hearn are thanked for providing constructive reviews of the submitted manuscript. The SEAL experiment was supported by ARC grant DP0342618. NR and MH are supported by ARC grants DP0556282 and DP0342618, respectively.

REFERENCES

ACHAUER U. 1994. New ideas on the Kenya rift based on the inversion of the combined dataset of the 1985 and 1989/90 seismic tomography experiments. *Tectonophysics* **236**, 305–329.

AKI K. A., CHRISTOFFERSSON A. & HUSEBYE E. S. 1977. Determination of the three-dimensional seismic structure of the lithosphere. *Journal of Geophysical Research* **82**, 277–296.

BALLING N. 2000. Deep seismic reflection evidence for ancient subduction and collision zones within the continental lithosphere of northwestern Europe. *Tectonophysics* **329**, 269–300.

BENZ H. M., ZANDT G. & OPPENHEIMER D. H. 1992. Lithospheric structure of northern California from teleseismic images of the upper mantle. *Journal of Geophysical Research* **97**, 4791–4807.

CALVERT A. J., SAWYER E. W., DAVIS W. J. & LUDDEN J. N. 1995. Archaean subduction inferred from seismic images of a mantle suture in the Superior Province. *Nature* **375**, 670–674.

CAMMARANO F., GOES S., VACHER P. & GIARDINI D. 2003. Inferring upper-mantle temperatures from seismic velocities. *Physics of the Earth and Planetary Interiors* **138**, 197–222.

CAYLEY R., TAYLOR D. H., VANDENBERG A. H. M. & MOORE D. H. 2002. Proterozoic–Early Palaeozoic rocks and the Tyennan Orogeny in central Victoria: the Selwyn Block and its tectonic implications. *Australian Journal of Earth Sciences* **49**, 225–254.

CLITHEROE G., GUDMUNDSSON O. & KENNETT B. L. N. 2000. The crustal thickness of Australia. *Journal of Geophysical Research* **105**, 13697–13713.

COOK F. A., VAN DER VELDEN A. J., HALL K. W. & ROBERTS B. J. 1999. Frozen subduction in Canada's Northwest Territories: lithoprobe deep lithospheric reflection profiling of the western Canadian Shield. *Tectonics* **18**, 1–24.

DEBAYLE E. & KENNETT B. L. N. 2000. The Australian continental upper mantle: structure and deformation inferred from surface waves. *Journal of Geophysical Research* **105**, 25423–25450.

FERGUSSON C. L. 2003. Ordovician–Silurian accretion tectonics of the Lachlan Fold Belt, southeastern Australia. *Australian Journal of Earth Sciences* **50**, 475–490.

FISHWICK S., KENNETT B. L. N. & READING A. M. 2005. Contrasts in lithospheric structure within the Australian craton—insights from surface wave tomography. *Earth and Planetary Science Letters* **231**, 163–176.

FOSTER D. A. & GRAY D. R. 2000. Evolution and structure of the Lachlan Fold Belt (Orogen) of eastern Australia. *Annual Reviews of Earth and Planetary Sciences* **28**, 47–80.

FREDERIKSEN A. W., BOSTOCK M. G., VAN DECAR J. C. & CASSIDY J. F. 1998. Seismic structure of the upper mantle beneath the northern Canadian Cordillera from teleseismic travel-time inversion. *Tectonophysics* **294**, 43–55.

GRAEBER F. M., HOUSEMAN G. A. & GREENHALGH S. A. 2002. Regional teleseismic tomography of the western Lachlan Orogen and Newer Volcanic Province, southeast Australia. *Geophysical Journal International* **149**, 249–266.

GRIFFIN W. L., O'REILLY S. Y., RYAN C. G., GAUL O. & IONOV D. A. 1998. Secular variation in the composition of subcontinental lithospheric mantle: geophysical and geodynamic implications. *In*: Braun J., Dooley J., Goleby B., van der Hilst R. & Klootwijk C. eds. *Structure and Evolution of the Australian Continent*, pp. 1–26. American Geophysical Union Geodynamic Series **26**.

HANSEN T. M. & BALLING N. 2004. Upper-mantle reflectors: modelling of seismic wavefield characteristics and tectonic implications. *Geophysical Journal International* **157**, 664–682.

HEARN S. J. & WEBB J. P. 1984. Relative teleseismic P residuals and upper mantle structure in eastern Queensland, Australia. *Seismological Society of America Bulletin* **74**, 1661–1681.

HUMPHREYS E. D. & CLAYTON R. W. 1990. Tomographic image of the southern California mantle. *Journal of Geophysical Research* **95**, 19725–19746.

KENNETT B. L. N. & ENGDAHL E. R. 1991. Travel times for global earthquake location and phase identification. *Geophysical Journal International* **105**, 429–465.

KENNETT B. L. N., ENGDAHL E. R. & BULAND R. 1995. Constraints on seismic velocities in the earth from travel times. *Geophysical Journal International* **122**, 108–124.

KENNETT B. L. N., SAMBRIDGE M. S. & WILLIAMSON P. R. 1988. Subspace methods for large scale inverse problems involving multiple parameter classes. *Geophysical Journal* **94**, 237–247.

LAWRENCE C. R. & ABELE C. 1988. Murray Basin. *In*: Douglas J. G. & Ferguson J. A. eds. *Geology of Victoria*, pp. 265–272. Geological Society of Australia, Victorian Division, Melbourne.

LIPPITSCH R., KISSLING E. & ANSORGE J. 2003. Upper mantle structure beneath the Alpine orogen from high-resolution teleseismic tomography. *Journal of Geophysical Research* **108**, 2376, doi: 10.1029/2002JB002016.

ONCESCU M. C., BURLACU V., ANGHEL M. & SMALLBERGHER V. 1984. Three-dimensional *P*-wave velocity image under the Carpathian Arc. *Tectonophysics* **106**, 305–319.

RAWLINSON N. & KENNETT B. L. N. 2004. Rapid estimation of relative and absolute delay times across a network by adaptive stacking. *Geophysical Journal International* **157**, 332–340.

RAWLINSON N., READING A. M. & KENNETT B. L. N. 2006. Lithospheric structure of Tasmania from a novel form of teleseismic tomography. *Journal of Geophysical Research* **111.**

RAWLINSON N. & SAMBRIDGE M. 2003. Seismic traveltime tomography of the crust and lithosphere. *Advances in Geophysics* **46**, 81–198.

RAWLINSON N. & SAMBRIDGE M. 2005. The fast marching method: an effective tool for tomographic imaging and tracking multiple phases in complex layered media. *Exploration Geophysics* **36**, 341–350.

SALTZER R. L. & HUMPHREYS E. D. 1997. Upper mantle *P* wave velocity structure of the eastern Snake River Plain and its relationship to geodynamic models of the region. *Journal of Geophysical Research* **102**, 11829–11841.

SIMONS F., ZIELHUIS A. & VAN DER HILST R. 1999. The deep structure of the Australian continent from surface wave tomography. *Lithos* **48**, 17–43.

SOBOLEV S. V., ZEYEN H., STOLL G., WERLING F., ALTHERR R. & FUCHS K. 1996. Upper mantle temperatures from teleseismic tomography of French Massif Central including effects of composition, mineral reactions, anharmonicity, anelasticity and partial melt. *Earth and Planetary Science Letters* **139**, 147–163.

SPAGGIARI C. V., GRAY D. R. & FOSTER D. A. 2004. Lachlan Orogen subduction–accretion systematics revisited. *Australian Journal of Earth Sciences* **51**, 549–553.

SPAGGIARI C. V., GRAY D. R., FOSTER D. A. & MCKNIGHT S. 2003. Evolution of the boundary between the western and central Lachlan Orogen: implications for Tasmanide tectonics. *Australian Journal of Earth Sciences* **50**, 725–749.

STECK L. K., THURBER C. H., FEHLER M., LUTTER W. J., ROBERTS P. M., BALDRIDGE W. S., STAFFORD D. G. & SESSIONS R. 1998. Crust and upper mantle P wave structure beneath Valles caldera, New Mexico: results from the Jemez teleseismic tomography experiment. *Journal of Geophysical Research* **103**, 24301–24320.

TAYLOR D. H. & CAYLEY R. A. 2000. Character and kinematics of faults within the turbidite-dominated Lachlan Orogen: implications for tectonic evolution of eastern Australia. Discussion. *Journal of Structural Geology* **22**, 523–528.

VANDENBERG A. H. M. 1999. Timing of orogenic events in the Lachlan Orogen. *Australian Journal of Earth Sciences* **46**, 691–701.

VANDENBERG A. H. M., WILLMAN C. E., MAHER S., SIMONS B. A., CAYLEY R. A., TAYLOR D. H., MORAND V. J., MOORE D. H. & RADOJKOVIC A. 2000. *The Tasman Fold Belt System in Victoria.* Geological Survey of Victoria Special Publication.

WILLMAN C. E., VANDENBERG A. H. M. & MORAND V. J. 2002. Evolution of the southeastern Lachlan Fold Belt in Victoria. *Australian Journal of Earth Sciences* **49**, 271–289.

ZIELHUIS A. & VAN DER HILST R. D. 1996. Mantle structure beneath the eastern Australia region from partitioned waveform inversion. *Geophysical Journal International* **127**, 1–16.

Received 28 July 2005; accepted 30 January 2006